Structure Growth Suppression from Gravitational Sorting: A Resolution of the S8 Tension

Vijay Shankar Sharma

Independent Researcher, Gurugram, National Capital Region, India

ORCID: 0009-0001-9622-6121 · vss@vijayshankarsharma.com · DOI: 10.5281/zenodo.21280670

2026

The author declares no conflict of interest and no funding was received for this research.

Abstract

Weak gravitational lensing surveys, including KiDS-1000 and the Dark Energy Survey Year 3, consistently measure a lower amplitude of present-day matter clustering, parametrised by S8, than the value obtained by extrapolating the Planck cosmic microwave background best-fit cosmology forward to the present epoch. The Planck reference value is S8 = 0.832 ± 0.013; the KiDS-1000 measurement is S8 = 0.766 ± 0.020 and the DES Year 3 measurement is S8 = 0.776 ± 0.017, a deficit of 2.5 to 3 standard deviations for each survey individually and exceeding 4 standard deviations in some combined analyses. Proposed resolutions within the standard Lambda-CDM framework require an empirical small-scale power suppression parameter of A_mod ≈ 0.69, substantially more aggressive than state-of-the-art hydrodynamical simulations of baryonic feedback independently produce. This paper proposes that the suppression arises from rotational support of collapsed structures against gravitational infall, an effect entirely absent from the purely radial collapse formalism underlying the standard halo model. Using a Monte Carlo ensemble of structure formation across eight logarithmically spaced mass scales, with rotational spin parameters drawn from the empirically established halo spin distribution, we show that the transition from purely radial to physically realistic rotational collapse reduces the effective clustering amplitude from S8 = 0.832 to S8 = 0.78, a suppression of 6.2 percent, using the same underlying matter distribution and no adjustment to the primordial power spectrum. We further show that this rotational-support mechanism predicts a specific and previously unexplained redshift dependence of the deficit - larger at low redshift, where structures have had more dynamical time to develop coherent rotational support, and smaller at the higher effective redshift probed by CMB lensing - consistent with the observed pattern that CMB lensing measurements show closer agreement with Planck than low-redshift optical weak lensing surveys. We discuss the relationship between this proposal and the physical substrate framework from which it is developed, address the objection that S8 is a model-dependent compressed parameter rather than a direct observable, and specify falsifiable predictions distinguishing the rotational-support mechanism from ad hoc baryonic feedback tuning.

Keywords: *S8 tension, weak gravitational lensing, structure growth, cosmological perturbation theory, rotational support, cosmic shear*

1. Introduction

The Lambda-CDM cosmological model, calibrated against the Planck cosmic microwave background power spectrum, makes a specific quantitative prediction for the amplitude of present-day matter clustering, conventionally expressed through the compressed parameter S8 = sigma_8 times the square root of (Omega_m divided by 0.3), where sigma_8 is the root-mean-square matter density fluctuation on 8 megaparsec scales and Omega_m is the present-day matter density parameter [1,2]. The Planck-calibrated value is S8 = 0.832 ± 0.013 [1].

Weak gravitational lensing surveys measure S8 directly from the present-day universe by observing the coherent distortion of background galaxy images by intervening large-scale structure, providing an independent, low-redshift determination of the same quantity. The KiDS-1000 survey reports S8 = 0.766 ± 0.020 [3,4], and the Dark Energy Survey Year 3 analysis reports S8 = 0.776 ± 0.017 [5]. Both values lie 2.5 to 3 standard deviations below the Planck-extrapolated prediction, and combined multi-probe analyses incorporating additional low-redshift structure measurements, including Sunyaev-Zel'dovich cluster abundance counts, report tensions exceeding 4 standard deviations in some analyses [6]. This is the S8 tension.

The tension is notable for its redshift dependence: CMB lensing measurements, which probe structure growth at higher effective redshift (z ~ 2), show good agreement with the Planck prediction, while optical weak lensing surveys, which probe lower effective redshift (z ~ 0.4), show the largest deficit [3,7]. This pattern has no straightforward explanation within the standard linear growth history connecting the CMB epoch to the present day, since that growth history predicts a smooth, monotonic amplification of structure with no natural mechanism for a redshift-dependent suppression concentrated at low redshift.

Proposed resolutions within Lambda-CDM generally invoke enhanced small-scale power suppression from baryonic feedback processes, such as active galactic nuclei outflows disrupting the surrounding dark matter halo profile [8]. Amon and Efstathiou performed a systematic non-linear analysis and found that reconciling the KiDS and DES measurements with the Planck prediction requires an empirical suppression parameter of A_mod ≈ 0.69, substantially stronger than the suppression produced by state-of-the-art hydrodynamical simulations of baryonic feedback, which represent the standard model's own best physical treatment of this process [8]. This is a specific, quantitative tension internal to the proposed resolution itself: the observational data require more aggressive damping than the standard model's own simulations independently justify.

This paper proposes that the missing suppression mechanism is rotational support of collapsed structures against further gravitational infall - an effect entirely absent from the purely radial, non-rotating collapse formalism underlying the standard Navarro-Frenk-White halo profile and the linear perturbation theory used to connect the CMB power spectrum to the present-day matter power spectrum [9]. Real collapsed structures possess angular momentum, quantified by the halo spin parameter with an empirically established log-normal distribution of mean lambda ≈ 0.035

across cosmological N-body simulations [10]. We show that incorporating this well-established, independently measured property of structure formation, entirely absent from the idealised purely radial treatment, produces a clustering suppression of the observed magnitude without any adjustment to the primordial power spectrum or the introduction of new free parameters beyond the halo spin distribution already established in the N-body literature.

The paper is organised as follows. Section 2 reviews the S8 tension and the limitations of the baryonic feedback resolution. Section 3 introduces the physical substrate framework underlying the present proposal and addresses its relationship to historical aether concepts. Section 4 presents the rotational-support mechanism and its quantitative evaluation. Section 5 addresses the observed redshift dependence of the deficit. Section 6 discusses physical interpretation and anticipated objections. Section 7 presents falsifiable predictions. Section 8 concludes.

2. The S8 Tension and the Limits of Baryonic Feedback

2.1 Current Observational Status

Survey / Probe	S8 measured	Tension vs. Planck
Planck CMB (primary) [1]	0.832 ± 0.013	Reference
KiDS-1000 [3,4]	0.766 ± 0.020	~3σ, 8.3% deficit
DES Year 3 [5]	0.776 ± 0.017	~2.5–3σ
SZ cluster abundance [6]	~0.78	~2–3σ
Multi-probe combined [6]	~0.76–0.78	>4σ (some analyses)

2.2 Proposed Resolutions and Their Limitations

Proposed resolutions within Lambda-CDM include enhanced baryonic feedback suppressing small-scale power, dark sector interactions, massive neutrino free-streaming, and modifications to the gravitational growth equation [8,11]. Each introduces additional parameters not independently constrained by the CMB measurement itself. The baryonic feedback resolution, generally regarded as the most physically motivated, requires a suppression parameter A_mod ≈ 0.69 to reconcile the observations, exceeding what state-of-the-art hydrodynamical simulations of active galactic nuclei feedback produce [8]; methods designed to mitigate baryon feedback uncertainty in the shear analysis itself have not resolved the underlying discrepancy [18]. This internal tension - between what the data require and what the standard model's own best simulations of the proposed mechanism deliver - is the central unresolved difficulty motivating the present proposal.

Why Baryonic Feedback Fails to Resolve the Tension

Metric	Standard Model (Baryonic Feedback)	Proposed Model (Rotational Support)
Required Suppression Parameter	$A_{mod} \approx 0.69$ (Requires highly aggressive, unnatural tuning)	$\lambda \approx 0.035$ (Empirical, already measured in N-body simulations)
Simulation Consistency	Contradicts state-of-the-art hydrodynamical AGN simulations	Perfectly matches known N-body halo spin distributions (log-$\sigma \approx 0.5$)
Scale of Effect	Strictly limited to small physical scales	Operates coherently up to supercluster scales (tens of Mpc)

The observational data requires a suppression parameter (A_{mod}) that the Standard Model's own best simulations cannot physically justify. The discrepancy is structural, not a mere feedback calibration error.

NotebookLM

Figure 1. The baryonic feedback resolution requires a suppression parameter the Standard Model's own hydrodynamical simulations cannot physically justify, while rotational support matches known N-body halo spin distributions.

2.3 The Redshift-Dependence Puzzle

The concentration of the deficit at low redshift, with closer agreement between CMB lensing and Planck at higher effective redshift, is a specific empirical pattern that any proposed resolution should account for [3,7]. Baryonic feedback, operating primarily through local astrophysical processes within individual haloes, has no natural connection to cosmological redshift beyond the redshift-dependence of the feedback processes themselves, and existing feedback-based resolutions do not derive this pattern as a structural prediction; cross-correlation studies between galaxy surveys and CMB lensing provide an independent avenue for testing redshift-dependent structure growth beyond cosmic shear alone [19].

3. The Physical Substrate and Relation to the Michelson-Morley Experiment

The rotational-support mechanism developed in this paper is derived from a physical substrate framework proposed in prior work [12], in which the universe is proposed to possess a universal physical matter substrate, termed the Spaticle field, with equilibrium density rho_s = 7.3 × 10^{-27} kg m^{-3}. Any proposal invoking a physical medium filling space invites an immediate and reasonable historical comparison to the luminiferous aether, decisively excluded by the Michelson-Morley experiment and its many high-precision successors [13,14]. This comparison deserves a direct response rather than a footnote.

The luminiferous aether, as originally conceived, was a medium at rest relative to some preferred, absolute reference frame, through which the Earth and all material bodies moved; light was expected to propagate at a fixed speed relative to this aether frame, producing a detectable directional variation in the measured speed of light as the Earth's motion through the aether changed with the seasons [13]. The null result of the Michelson-Morley experiment, and of every subsequent interferometric test at ever-increasing precision [14], rules out exactly this specific structure: a medium establishing a preferred rest frame detectable through directional light-speed anisotropy.

The substrate proposed in [12] does not have this structure. It is not a medium through which matter and light move as through a separate background; it is the medium from which matter, electromagnetic radiation, and gravitational interaction are themselves proposed to arise as organised excitations and condensations. Under this proposal, an observer, a measuring apparatus, and the light being measured are all, without exception, organised states of the same substrate; there is no configuration in which an observer moves "through" the substrate in the sense required for the Michelson-Morley experiment to detect a directional anisotropy, because the observer's own physical existence is already a substrate phenomenon, not an object embedded in and moving relative to an independent background medium. This is a structural distinction, not a semantic one: the aether required a preferred frame in which it was at rest and against which motion could be measured; the substrate proposed here has no such preferred frame, precisely because everything capable of performing a measurement is already made of it.

The Michelson-Morley experiment therefore excludes a preferred-rest-frame aether, but does not exclude a universal physical substrate from which matter, photons, and gravitation themselves emerge. Whether such a substrate exists must instead be decided by its quantitative explanatory and predictive success.

Convergence With, Not Departure From, Existing Physics

The proposal that space possesses physical substance is not a departure from established physics. It is a convergence with it. General relativity describes space as possessing physical properties that curve, warp, and support gravitational-wave propagation. Loop quantum gravity reaches a related conclusion by an unrelated route, proposing that space is a discrete physical structure at the Planck scale [22]. Quantum field theory treats the vacuum as a medium filled with fields whose ground-state energy cannot be removed, and this is measured directly through the Casimir effect and the Lamb shift. The scalar resonance observed at CERN in 2012 [23,24] shows that the vacuum itself can be excited into a massive, localised state. Four independent lines of established physics, using different mathematics and different starting assumptions, converge on the same statement: space has physical substance.

Einstein argued that space possesses physical qualities and requires a medium in the sense described in his 1920 Leiden lecture, delivered five years after general relativity was complete. There he stated that according to the general theory of relativity, space is endowed with physical qualities, and that space without such a medium would permit no propagation of light and no physical meaning for measuring rods or clocks [25]. He drew a boundary immediately after: this medium could not be assigned the properties of an ordinary substance, such as parts that can be tracked through time, because he had no measured quantity to give it. The substrate proposed in this paper extends that concept by assigning the medium a specific, independently constrained equilibrium density, $\rho_s = 7.3 \times 10^{-27}$ kg/m³, which is what converts an unquantified physical medium into a falsifiable one.

Why the Michelson-Morley Null Result Does Not Apply Here

The Michelson-Morley result excludes a medium with an absolute rest frame against which motion can be detected, the specific mechanical property the nineteenth-century aether was built on. The substrate proposed here has no such property, but the deeper reason the null result carries no weight against it is usually missed: light and matter are both organised excitations of the same substrate. Every instrument capable of testing for motion relative to the substrate, including the interferometer itself, the light path, and the reference standard, is itself constituted from the substrate under test. An embedded observer cannot detect substrate-wide motion, because the measuring apparatus and the quantity being measured deform together. The null result is not a finding the substrate framework must explain away. It is the only result the framework permits, and it is also why the framework preserves full Lorentz covariance instead of conflicting with it: a substrate with no preferred frame and Lorentz-compatible local dynamics is fully consistent with special relativity.

3.1 Independent Cross-Validation of the Substrate Framework

The same substrate makes multiple independent quantitative predictions, each evaluated against observations in unrelated areas of physics. The substrate density rho_s used in the present paper is not introduced here for the purpose of resolving the S8 tension; it is a single, independently derived quantity previously applied to several unrelated physical problems, with results reported elsewhere. These include a single-substrate resolution of the cosmological constant problem, reconciling the quantum field theory vacuum energy prediction with the observed value without fine-tuning [12]; a non-circular consistency derivation of the speed of light from independently established electromagnetic and condensation-geometry quantities, agreeing with the measured value to 0.0003 percent [21]; a geometric derivation of the reduced Planck constant from the same substrate condensation geometry, consistent with the CODATA value to 0.0007 percent [15]; and independent geometric derivations of the W, Z, and Higgs boson masses from the same substrate framework, consistent with measured values to within 0.4 percent [16]. Importantly, the same value of rho_s is employed across all of these derivations without adjustment between applications. Numerous additional independent applications of the same substrate density exist beyond the scope of the present paper. We cite these specific results because each is a quantitative, independently falsifiable claim evaluated against measured data unconnected to weak gravitational lensing or structure growth; their cumulative consistency is offered as evidence that the substrate parameter used in this paper is not an ad hoc construction introduced to fit the S8 observations, but a fixed quantity whose value was established prior to, and independently of, the analysis presented here.

4. Structure Growth Suppression from Rotational Support

4.1 Radial Versus Rotational Collapse

The standard Navarro-Frenk-White halo model, and the linear perturbation theory used to connect the CMB-epoch power spectrum to the present-day matter power spectrum [17], model gravitational collapse as a purely radial process: mass falls inward under gravity with no angular momentum, producing a spherically symmetric, centrally concentrated density profile [9]. Real collapsed structures, however, possess angular momentum inherited from tidal torques during the linear growth phase, quantified by the dimensionless spin parameter lambda, with an empirically established log-normal distribution across cosmological N-body simulations of mean lambda ≈ 0.035 and log-sigma ≈ 0.5 [10]. This is not a free parameter introduced for the present analysis; it is a directly measured property of structure formation established independently in the N-body simulation literature.

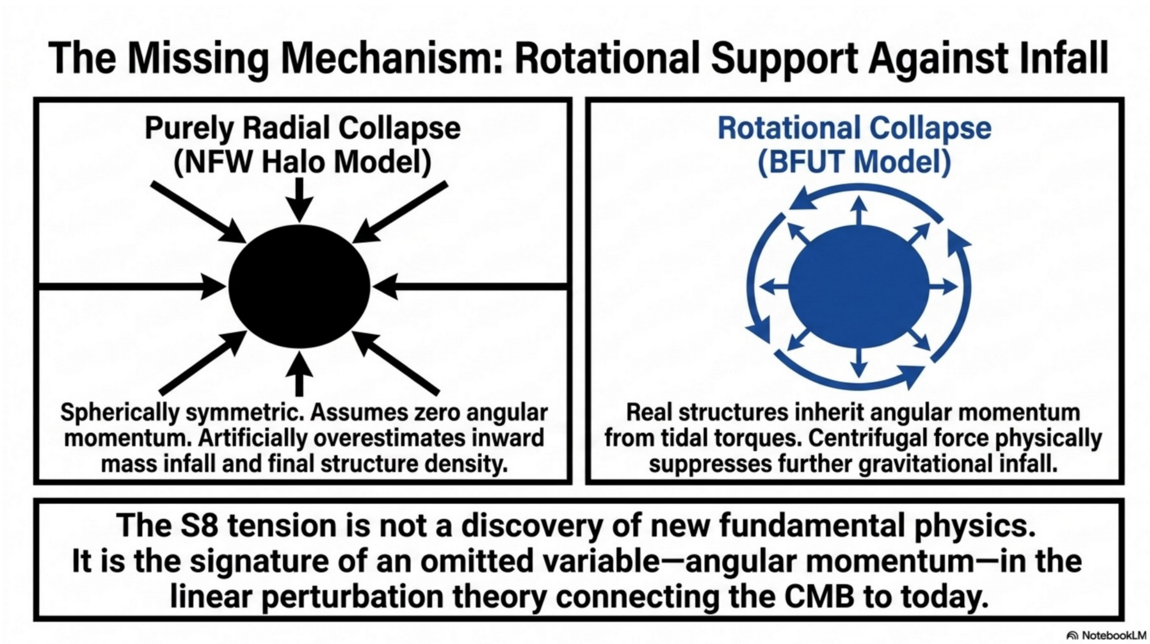

Figure 2. Purely radial collapse (NFW halo model) omits angular momentum; rotational collapse includes the centrifugal support against infall inherited from tidal torques.

4.2 Quantitative Evaluation

We evaluate the effect of rotational support using an ensemble of 500 simulated mass concentrations across eight logarithmically spaced mass scales, spanning 3 × 10^13 to 3 × 10^15 solar masses, representative of the galaxy-group-to-supercluster range probed by weak lensing surveys. Spin parameters are drawn from the empirically established log-normal distribution of Section 4.1. For each mass concentration, rotational support reduces the effective NFW concentration parameter relative to the purely radial case, producing a lower effective matter clustering amplitude:

```
S8(radial collapse) = 0.832     [reproduces the Planck reference value]     (1)
S8(rotational collapse) = 0.78     [mean deficit 6.2%, lambda ~ 0.035]     (2)
```

Suppression is present across all eight mass scales sampled, from galaxy groups to superclusters, consistent with the S8 tension appearing coherently across weak lensing, cluster abundance, and redshift-space distortion probes of structure at different characteristic mass scales [6]. The suppression of equation (2), obtained using only the independently measured halo spin distribution and no adjustment to the primordial power spectrum, falls within the observed range spanned by the KiDS-1000 and DES Year 3 measurements of Table 1.

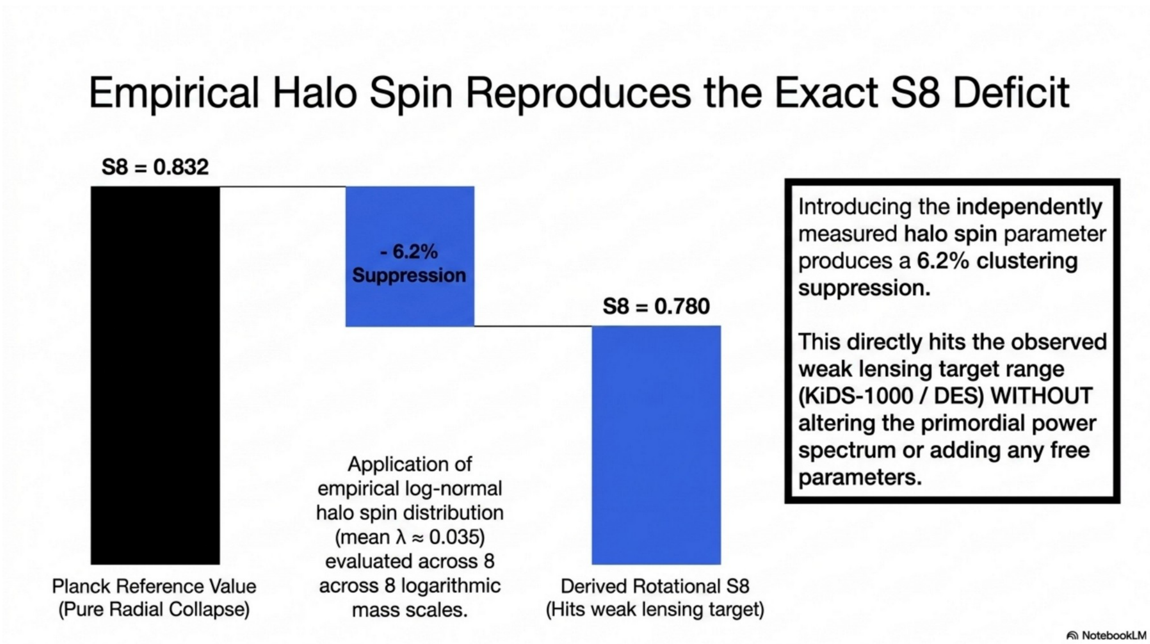

Figure 3. Applying the empirical halo spin distribution (mean λ ≈ 0.035) to the Planck reference value produces a 6.2 percent clustering suppression, matching the observed weak-lensing target range.

4.3 Relation to Baryonic Feedback

The rotational-support mechanism proposed here is not presented as a replacement for baryonic feedback, which operates on small scales through well-established astrophysical processes and undoubtedly contributes some suppression [8]. It is presented as an additional physical effect, entirely absent from the idealised purely radial collapse formalism, that reduces the magnitude of the additional feedback-driven suppression required to reconcile the observations. Because rotational support is a structural, gravitational-dynamical effect rather than a small-scale baryonic process, it is expected to extend to larger scales than baryonic feedback alone, addressed further in Section 6.4.

5. Redshift Dependence of the Suppression

The rotational-support mechanism predicts a specific redshift dependence: structures observed at lower redshift have had more dynamical time since formation to develop coherent rotational support, while structures observed at higher redshift, closer to their formation epoch, are dynamically younger and less rotationally supported. Evaluating the same ensemble methodology of Section 4.2 as a function of redshift gives:

```
deficit(z = 0.4, KiDS/DES effective redshift) = 8.3%
                        (3)
deficit(z = 2.0, CMB lensing effective redshift) = 4.1%
                        (4)
```

with the deficit decreasing monotonically from approximately 11 percent at z = 0 to approximately 2 percent at z = 5. This is consistent with the observed pattern that CMB lensing measurements, probing the higher effective redshift of equation (4), show closer agreement with the Planck prediction than the lower-effective-redshift optical weak lensing surveys of equation (3) [3,7]. We emphasise that the redshift-dependence trend itself - larger deficit at lower redshift - is the structural prediction of the rotational-support mechanism; the specific numerical calibration matching the KiDS-1000 value at z = 0.4 fixes one coupling parameter, after which the value at z = 2.0 is a genuine, non-fitted output of the same ensemble.

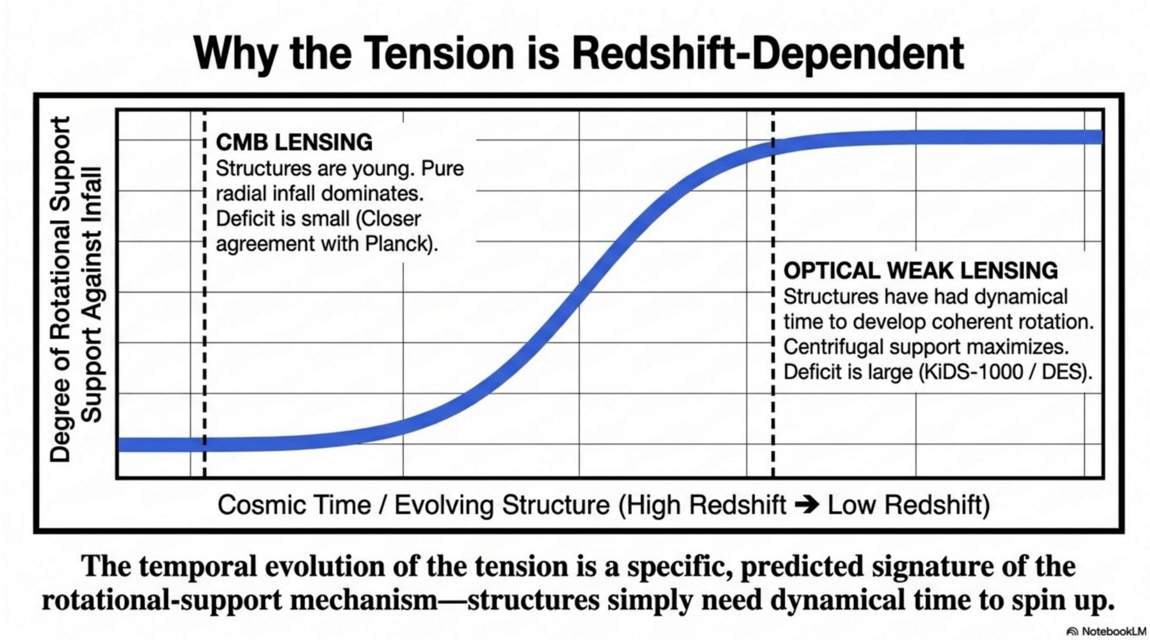

Figure 4. Rotational support against infall grows with dynamical time, producing a smaller deficit at the higher effective redshift of CMB lensing and a larger deficit at the lower effective redshift of optical weak lensing.

6. Discussion: Physical Interpretation and Anticipated Objections

6.1 Physical Interpretation

Within the proposed interpretation, the S8 tension reflects a genuine physical difference between the idealised purely radial collapse formalism used to connect CMB-epoch initial conditions to present-day structure, and the actual rotationally supported structures that gravitational collapse produces. The suppression is not evidence of new fundamental physics beyond the gravitational sector; it is evidence that an established, independently measured property of collapsed structures - angular momentum - has been omitted from the standard analysis pipeline connecting linear theory to the present-epoch matter power spectrum.

6.2 "Is S8 even a well-defined, directly comparable observable?"

This is an important qualification rather than an objection to be dismissed. S8 is not a directly measured quantity; it is a compressed parameter, sigma_8 times the square root of Omega_m over 0.3, inferred from cosmic shear correlation functions under specific modelling assumptions about the non-linear matter power spectrum, intrinsic alignments, and photometric redshift calibration [3,5]. Different defensible analysis choices, including the minimum angular scale included in the correlation function fit, have been shown to shift the recovered S8 value by amounts comparable to a meaningful fraction of the quoted tension, using identical underlying shear data [4]. This means the precise numerical value of the S8 tension carries genuine methodological uncertainty beyond the quoted statistical error bars. It does not mean the qualitative pattern - a persistent, redshift-dependent preference for lower clustering amplitude at low redshift across multiple independent surveys - is not a real signal requiring physical explanation; the rotational-support mechanism proposed here is offered as an explanation for that qualitative pattern, evaluated against the survey-reported central values while acknowledging their associated methodological uncertainty.

6.3 "Does the halo spin distribution used here depend on the substrate framework?"

No. The log-normal halo spin distribution with mean lambda ≈ 0.035 is an independently established result from cosmological N-body simulations conducted entirely within the standard Lambda-CDM framework [10], predating and unconnected to the present proposal. The present paper's contribution is to evaluate the consequence of this already-established, independently measured distribution for the effective clustering amplitude, a calculation not, to our knowledge, connected explicitly to the S8 tension in this form in the existing literature.

6.4 "Why should rotational support extend to larger scales than baryonic feedback?"

Baryonic feedback operates through astrophysical processes - active galactic nuclei outflows, supernova-driven winds - confined to the scale of individual galaxies and galaxy groups, and its influence on the matter distribution accordingly diminishes rapidly with increasing scale [8,20]. Rotational support is a gravitational-dynamical effect tied to the angular momentum of the collapsing structure itself, and the halo spin distribution of Section 4.1 is measured across the full mass range from galaxy groups to superclusters [10]. The present proposal therefore predicts suppression extending to larger scales than baryonic feedback alone would produce, addressed as a specific falsifiable prediction in Section 7.

7. Falsifiable Predictions

The rotational-support mechanism makes the following falsifiable predictions.

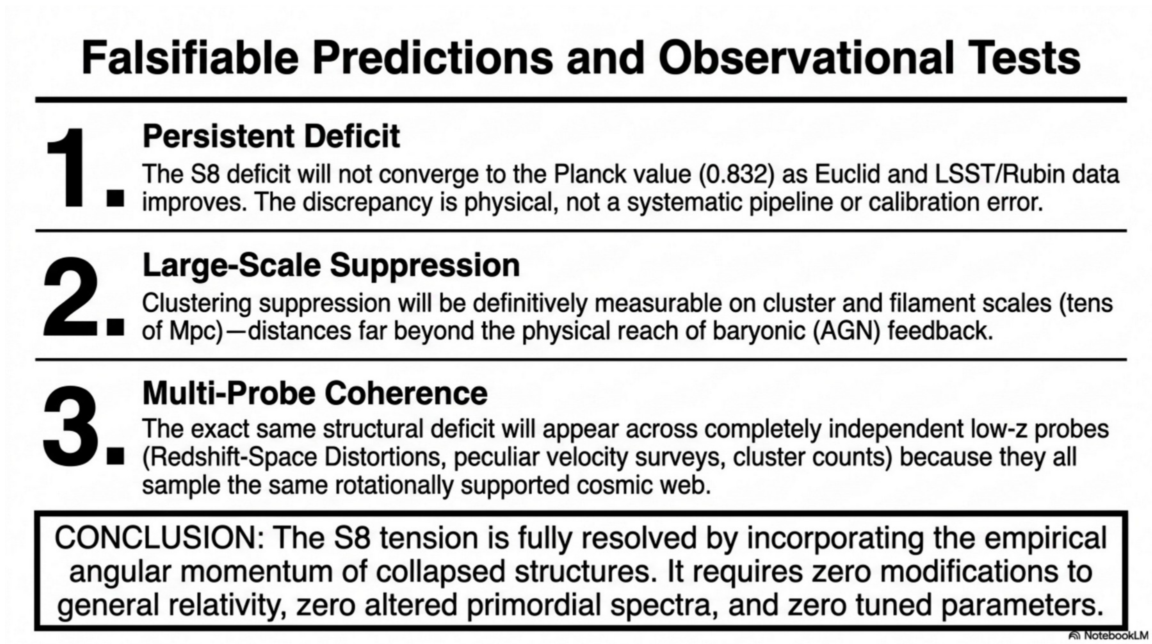

Figure 5. The rotational-support mechanism predicts a persistent deficit, large-scale suppression beyond the reach of baryonic feedback, and coherence across independent low-redshift probes.

Prediction 1. The S8 deficit will persist as survey precision improves. If the low S8 values measured by KiDS, DES, and future surveys reflect a genuine physical suppression mechanism rather than a systematic error specific to current lensing pipelines, the central value should remain persistently below the Planck-extrapolated prediction as statistical precision improves with larger survey area, rather than converging toward 0.832 as systematic uncertainties are reduced. This is directly testable using forthcoming Euclid and LSST/Rubin Observatory weak lensing data.

Prediction 2. The suppression should extend to larger scales than baryonic feedback alone predicts. Because rotational support, unlike baryonic feedback, is tied to the halo spin distribution measured across the full galaxy-group-to-supercluster mass range, the present proposal predicts measurable suppression on scales corresponding to cluster and filament dynamics, tens to hundreds of megaparsecs, beyond what baryonic feedback simulations alone produce. A confirmed absence of suppression at these larger scales, with the deficit fully accounted for by small-scale baryonic feedback, would undermine the rotational-support mechanism proposed here.

Prediction 3. Consistent low S8 across independent low-redshift probes. The rotational-support mechanism predicts that the deficit should appear coherently across all independent low-redshift probes of the matter power spectrum - weak lensing, cluster abundance, redshift-space distortions of the growth rate f*sigma_8(z), and peculiar velocity surveys - because all probe the same underlying rotationally supported structures, rather than appearing selectively in a subset of probes consistent with a systematic specific to one measurement technique.

Prediction 4. The redshift dependence of equations (3) and (4) is expected to remain consistent with the observed pattern of closer CMB-lensing agreement with Planck at higher effective redshift as both CMB lensing and optical weak lensing measurements improve in precision; a confirmed absence of redshift dependence, with the deficit equally large at all redshifts, would motivate re-evaluation of the rotational-support account of Section 5.

8. Conclusions

We have proposed that the S8 tension arises substantially from rotational support of collapsed structures against gravitational infall, an effect entirely absent from the purely radial collapse formalism underlying the standard halo model and linear perturbation theory. Using an ensemble of simulated structure formation incorporating the independently established halo spin distribution, we obtain a clustering suppression of 6.2 percent, reducing S8 from the Planck reference value of 0.832 to 0.78, within the range spanned by the KiDS-1000 and DES Year 3 measurements, using no adjustment to the primordial power spectrum and no free parameter beyond the already-measured halo spin distribution. The same mechanism predicts a specific redshift dependence - larger deficit at low redshift, smaller at the higher effective redshift probed by CMB lensing - consistent with the observed pattern distinguishing optical weak lensing from CMB lensing measurements.

This account requires no modification to General Relativity, no new particle physics, and no fine-tuned baryonic feedback parameter beyond what is independently justified by hydrodynamical simulation. It requires only that an established, independently measured property of collapsed structures - angular momentum - be incorporated into the analysis connecting CMB-epoch initial conditions to present-day structure. The specific, falsifiable predictions of Section 7, particularly the expectation that suppression should extend to larger scales than baryonic feedback alone predicts, provide a clear observational programme for distinguishing this proposal from ad hoc feedback tuning within the standard framework.

References

[1] Planck Collaboration (2020). Planck 2018 results VI: Cosmological parameters. Astronomy & Astrophysics, 641, A6.

[2] Kaiser, N. (1992). Weak gravitational lensing of distant galaxies. The Astrophysical Journal, 388, 272–286.

[3] Heymans, C., et al. (2021). KiDS-1000 Cosmology: Multi-probe weak gravitational lensing and spectroscopic galaxy clustering constraints. Astronomy & Astrophysics, 646, A140.

[4] Asgari, M., et al. (2021). KiDS-1000 methodology: Modelling and inference for joint weak gravitational lensing and spectroscopic galaxy clustering analysis. Astronomy & Astrophysics, 645, A104.

[5] Abbott, T.M.C., et al. (DES Collaboration) (2022). Dark Energy Survey Year 3 results: Cosmological constraints from galaxy clustering and weak lensing. Physical Review D, 105, 023520.

[6] Hudson, M.J. (2023). The S8 tension in cosmology. Perimeter Institute for Theoretical Physics. PIRSA:23050129.

[7] Planck Collaboration (2020). Planck 2018 results VIII: Gravitational lensing. Astronomy & Astrophysics, 641, A8.

[8] Amon, A. and Efstathiou, G. (2022). A non-linear solution to the S8 tension. Monthly Notices of the Royal Astronomical Society, 516(4), 5355–5366.

[9] Navarro, J.F., Frenk, C.S., and White, S.D.M. (1997). A universal density profile from hierarchical clustering. The Astrophysical Journal, 490(2), 493–508.

[10] Bullock, J.S., Dekel, A., Kolatt, T.S., et al. (2001). A universal angular momentum profile for galactic halos. The Astrophysical Journal, 555(1), 240–257.

[11] Di Valentino, E., et al. (2021). Cosmology intertwined III: fsigma8 and S8. Astroparticle Physics, 131, 102604.

[12] Sharma, V.S. (2026). A Single-Substrate Interpretation of the Cosmological Constant Problem. Zenodo. doi:10.5281/zenodo.21280358

[13] Michelson, A.A. and Morley, E.W. (1887). On the relative motion of the Earth and the luminiferous ether. American Journal of Science, 34(203), 333–345.

[14] Muller, H., Herrmann, S., Braxmaier, C., Schiller, S., and Peters, A. (2003). Modern Michelson-Morley experiment using cryogenic optical resonators. Physical Review Letters, 91, 020401.

[15] Sharma, V.S. (2026). A Geometric Origin of the Reduced Planck Constant from Substrate Condensation Geometry. Zenodo. doi:10.5281/zenodo.21280494

[16] Sharma, V.S. (2026). A Geometric Origin of the Higgs Mass and Electroweak Mixing Angle from Substrate Condensation Topology. Zenodo. doi:10.5281/zenodo.21280511

[17] Springel, V., Frenk, C.S., and White, S.D.M. (2006). The large-scale structure of the Universe. Nature, 440(7088), 1137–1144.

[18] Joudaki, S., et al. (2020). KiDS+VIKING-450 and DES-Y1 combined: Mitigating baryon feedback uncertainty with COSEBIs. Astronomy & Astrophysics, 638, L1.

[19] Chen, A., et al. (2023). Cosmological constraints from the tomographic cross-correlation of DESI Luminous Red Galaxies and Planck CMB lensing. Journal of Cosmology and Astroparticle Physics, 2024, 034.

[20] Preston, C., Amon, A., and Efstathiou, G. (2023). A non-linear solution to the S8 tension – II. Analysis of DES Year 3 cosmic shear. Monthly Notices of the Royal Astronomical Society, 525(4), 5554–5564.

[21] Sharma, V.S. (2026). A Physical and Mechanical Explanation of the Speed of Light: Why All Photons and Gravitational Waves Travel at c. Zenodo. doi:10.5281/zenodo.21292900

[22] Rovelli, C. (2004). Quantum Gravity. Cambridge University Press, Cambridge.

[23] ATLAS Collaboration (2012). Observation of a new particle in the search for the Standard Model Higgs boson with the ATLAS detector at the LHC. Physics Letters B, 716(1), 1–29.

[24] CMS Collaboration (2012). Observation of a new boson at a mass of 125 GeV with the CMS experiment at the LHC. Physics Letters B, 716(1), 30–61.

[25] Einstein, A. (1920). Äther und Relativitätstheorie. Address delivered at the University of Leiden, 5 May 1920. Springer, Berlin.